



Prediction of pile settlement using artificial neural networks based on standard penetration test data

F. Pooya Nejad^a, Mark B. Jaksa^{b,*}, M. Kakhi^a, Bryan A. McCabe^c

^a Dept. of Civil Engineering, Ferdowsi University of Mashhad, Mashhad, Iran

^b School of Civil, Environmental and Mining Engineering, University of Adelaide, Australia

^c Dept. of Civil Engineering, National University of Galway, Ireland

ARTICLE INFO

Article history:

Received 30 June 2008

Received in revised form 12 March 2009

Accepted 21 April 2009

Available online 20 May 2009

Keywords:

Pile load test

Pile foundation

Settlement

Neural networks

ABSTRACT

In recent years artificial neural networks (ANNs) have been applied to many geotechnical engineering problems with some degree of success. With respect to the design of pile foundations, accurate prediction of pile settlement is necessary to ensure appropriate structural and serviceability performance. In this paper, an ANN model is developed for predicting pile settlement based on standard penetration test (SPT) data. Approximately 1000 data sets, obtained from the published literature, are used to develop the ANN model. In addition, the paper discusses the choice of input and internal network parameters which were examined to obtain the optimum model. Finally, the paper compares the predictions obtained by the ANN with those given by a number of traditional methods. It is demonstrated that the ANN model outperforms the traditional methods and provides accurate pile settlement predictions.

© 2009 Elsevier Ltd. All rights reserved.

1. Introduction

In deep foundation systems, piles are part of the sub-structure which are intended to transfer the structural loads through a soft or otherwise unsuitable stratum onto one which is firmer at depth. The design of pile foundations must consider constructability, and must meet strength and serviceability criteria like most civil engineering systems. In order to satisfy serviceability, it is essential that reliable predictions of pile settlement are available.

Settlement occurs as a consequence of an increase in effective stress causing a volume reduction of the subsoil. It is the sum of: (i) elastic compression of the soil skeleton, which occurs quickly and is normally small, and (ii) consolidation or volume change due to the expulsion of water, which occurs quickly in coarse-grained soils but slowly in fine-grained soils.

Soil materials typically do not show a linear relationship between stress and strain and settlement is a function of the relative vertical stress increase. In conventional approaches, the settlement is calculated by dividing the soil profile into layers and calculating for each layer the compression caused by the stress increase. The settlement is then equal to the sum of the compression of the individual layers [9].

The problem of estimating pile settlement is very complex and not yet entirely understood. This can be attributed, at least in part, to the uncertainty associated with the factors that affect the

magnitude of this settlement. These factors include the distribution of applied stress, stress-strain history of the soil, soil compressibility, and difficulty in obtaining undistributed samples of soil [37]. There are many methods in the geotechnical literature, both theoretical and experimental, for predicting the settlement of piles. Due to the difficulty of obtaining undisturbed samples, many settlement prediction methods have focused on correlations with in situ tests, such as the cone penetration test (CPT), standard penetration test (SPT), and dilatometer test.

However, most of the available methods simplify the problem by incorporating several assumptions associated with the aforementioned factors that affect the settlement of piles. Consequently, most of the existing methods fail to achieve consistent success in relation to accurate settlement prediction [32]. As a result, alternative methods are needed, which provide more accurate settlement prediction.

In recent times, artificial neural networks (ANNs) have been applied to many geotechnical engineering problems and have demonstrated some degree of success. ANNs are a form of artificial intelligence, which, by means of their architecture, attempt to simulate the biological structure of the human brain and nervous system. Although the concept of artificial neurons was first introduced in 1943, research into applications of ANNs has blossomed since the introduction of the back propagation training algorithm for feed forward ANNs in 1986 [35]. ANNs may thus be considered a relatively new tool in the field of prediction and forecasting.

In this paper, ANNs are used to predict the settlement of piles base on standard penetration test (SPT) data. The aims of the paper are:

* Corresponding author.

E-mail address: mark.jaksa@adelaide.edu.au (M.B. Jaksa).

Nomenclature

| | | | |
|------------------------|---|----------------|---|
| A_{tip} | cross-sectional area of the pile tip | O | perimeter of pile |
| C_p, C_s | empirical coefficients | P | applied load |
| C_N | adjustment for effective overburden pressure | P_w | working load applied to the pile |
| $C_{y_j d_j}$ | covariance between the model output (y_j) and the desired output (d_j) | P_{wp} | load carried at the pile tip under working load conditions |
| d | diameter, or width, of the pile | P_{ws} | the load carried by skin resistance |
| d_j | desired (observed) output | q_p | ultimate tip resistance of the pile |
| \bar{d} | mean of the desired output d_j | R_h | correction factor for finite depth of a layer on a rigid base |
| E | Young's modulus of elasticity of the pile material | R_k | correlation factor for pile compressibility |
| EA | axial rigidity of pile | R_v | correlation factor for Poisson's ratio of soil |
| E_s | Young's modulus of elasticity of the soil | s | calculated settlement |
| I | influence factor for a rigid pile in a deep layer | s_m | measured settlement |
| I_0 | settlement-influence factor for pile compressibility | s_1 | pile settlement due to the pile shaft |
| I_ρ, I_{ρ_s} | empirical coefficients | s_2 | pile settlement due to the tip load |
| L | length of pile | s_3 | pile settlement due to the skin friction load |
| L_{embed} | embedded length of pile | y_j | model (predicted) output |
| N_1, N_2, \dots, N_5 | average corrected standard penetration test blow count/300 mm along the first, second, third, fourth and fifth segments along the embedded length of the pile | \bar{y} | mean of the model output y_j |
| N_{avej} | average corrected standard penetration test blow count/300 mm along the embedded length of pile for layer j | Z_i | the soil layer thickness |
| N_{tip} | average corrected standard penetration test blow count/300 mm at the pile tip to the depth of influence | ν | Poisson's ratio of the soil |
| n | number of data | σ_{d_j} | standard deviation of the desired output d_j |
| | | σ'_v | effective overburden pressure |
| | | σ_{y_j} | standard deviation of the model output y_j |
| | | ζ | factor dependent on the unit skin friction distribution |

- To develop an ANN model for accurately predicting the settlement of single, axially-loaded piles.
- To study the effect of ANN geometry and some internal parameters on the performance of ANN models.
- To explore the relative importance of the factors affecting settlement prediction by carrying out sensitivity analysis.
- To compare the performance of the ANN model with four of the most commonly used traditional methods.

2. Development of neural network model

The development of ANN models requires the determination of model inputs and outputs, division and pre-processing of the available data, the determination of appropriate network architecture,

Table 1
Database references.

| Reference | Location of test(s) | No. of pile load tests |
|---|------------------------|------------------------|
| Al-Homoud et al. [1] | Sharje, UAE | 1 |
| Altaee et al. [2] | Baghdad, Iraq | 2 |
| Balakrishnan et al. [3] | Kuala Lumpur, Malaysia | 11 |
| Briaud et al. [5] | Texas A&M University | 2 |
| Broms and Hellman [6] | Sweden | 1 |
| Farquhar [10] | Auckland, New Zealand | 1 |
| Florida Department of Transportation [13] | USA | 27 |
| Hirayama [17] | Japan | 3 |
| Ismael [19] | Kuwait | 3 |
| Keller, unpublished | Ashford, UK | 2 |
| Keller, unpublished | Imperial Wharf, UK | 3 |
| Lin et al. [22] | Taiwan | 2 |
| Lo and Li [23] | Hong Kong | 2 |
| Ng et al. [29] | Hong Kong | 1 |
| Omer et al. [30] | Cardiff, UK | 5 |
| Paik and Salgado [31] | Indiana, US | 2 |
| US Dept. of Transportation [43] | Virginia, US | 4 |
| Yang et al. [46] | Hong Kong | 2 |
| Zhang et al. [47] | Hong Kong | 2 |

stopping criteria, and model validation [37]. The personal computer-based software *NEUFRAME* version 4.0 (Neurosciences Corp. 2000) is used to simulate ANN operation in this work.

The data used to calibrate and validate the neural network model were obtained from both published literature and the authors own files. Suitable case studies were those having pile load tests that include field measurements of full-scale pile settlements, as well as the corresponding information regarding the piles and soil. The database contains a total of 1013 cases from 76 individual pile load tests. The references used to compile the database are given in Table 1.

3. Model inputs and outputs

In order to obtain accurate settlement predictions, a thorough understanding of the factors affecting settlement is needed [37]. Most traditional pile settlement methods include the following fundamental parameters: pile geometry, pile material properties, applied load and soil properties. There are some additional factors, such as the pile installation type, load test method, whether the pile tip is closed or open, and the depth to the water table. The depth of water table is not included in this study, as it is believed that its effect is already accounted for in the measured SPT blow count [26].

Since settlement depends on the soil compressibility and the SPT is one of the most commonly used tests in practice for indicating the in situ compressibility of soils; the SPT blow count/300 mm (N) along the embedded length of the pile is used as a measure of soil compressibility for the purpose of this study. To account more accurately for the variability of soil properties along the shaft of the pile, the embedded length of the pile is divided into five segments of equal thickness, with each being an average of N over that segment. The average N count, N_{avej} , for each subdivision, j , is calculated as below [4]:

$$N_{avej} = \frac{\sum N_i Z_i}{\sum Z_i}$$

where, Z_i is the soil layer thickness in that segment with N_i over that layer.

In addition, as suggested by Liao and Whitman [21], for sand the value of N_{avej} for each subdivision is corrected for overburden pressure, as given below. This correction is not used for clays

$$N_{correctj} = C_N \times N_{avej}$$

$$C_N = \sqrt{\frac{95.76}{\sigma'_v}}$$

where, C_N is the adjustment for effective overburden pressure; and σ'_v is the effective overburden pressure (kPa).

Hence, the factors that are presented to the ANN as model input variables are the: (i) type of pile load test (maintained load or constant rate of penetration); (ii) pile material (concrete, steel, composite and plastic); (iii) method of installation (replacement or displacement); (iv) pile tip (closed or open); (v) axial rigidity of the pile (EA); (vi) cross sectional area of the pile tip (A_{tip}); (vii) perimeter of the pile in contact with the soil (O); (viii) length of the pile (L); (ix) embedded length of the pile (L_{embed}); (x) the averaged and corrected SPT blow count/300 mm along the embedded length of the pile (N_1, N_2, N_3, N_4, N_5); (xi) the corrected SPT blow count/300 mm at the tip of the pile (N_{tip}) and (xii) applied load (P). Pile settlement is the single output variable.

Table 2
Artificial neural network input and output statistics.

| Model variables and data sets | Statistical parameters | | | | |
|---|------------------------|------------------------|-----------|---------|-----------|
| | Mean | Std. Dev. ^a | Maximum | Minimum | Range |
| <i>Axial rigidity of pile, EA (MN)</i> | | | | | |
| Training set | 22095.02 | 25178.04 | 247400.40 | 1692.04 | 245708.34 |
| Testing set | 20976.07 | 13636.90 | 109955.70 | 1692.04 | 108263.66 |
| Validation set | 20628.17 | 12016.72 | 58240.00 | 1692.04 | 56547.96 |
| <i>Cross sectional area of pile tip, A_{tip} (cm²)</i> | | | | | |
| Training set | 5080.32 | 7761.74 | 70685.83 | 229.30 | 70456.53 |
| Testing set | 5141.46 | 4574.68 | 31415.93 | 229.30 | 31186.63 |
| Validation set | 5211.19 | 4269.01 | 22400.00 | 229.30 | 22170.70 |
| <i>Perimeter of pile, O (cm)</i> | | | | | |
| Training set | 563.27 | 273.59 | 1137.10 | 78.54 | 1058.56 |
| Testing set | 574.65 | 268.07 | 1137.10 | 78.54 | 1058.56 |
| Validation set | 540.98 | 268.75 | 1137.10 | 78.54 | 1058.56 |
| <i>Length of pile, L (m)</i> | | | | | |
| Training set | 32.63 | 14.21 | 81.10 | 8.24 | 72.86 |
| Testing set | 30.44 | 14.75 | 81.10 | 8.24 | 72.86 |
| Validation set | 29.40 | 15.39 | 81.10 | 8.24 | 72.86 |
| <i>Embedded length of pile, L_{embed} (m)</i> | | | | | |
| Training set | 25.99 | 13.20 | 81.10 | 6.45 | 74.65 |
| Testing set | 23.01 | 14.23 | 81.10 | 6.45 | 74.65 |
| Validation set | 22.49 | 14.66 | 81.10 | 6.45 | 74.65 |
| <i>Average SPT blow, N₁ (Corrected)</i> | | | | | |
| Training set | 14.61 | 23.38 | 161.00 | 0.00 | 161.00 |
| Testing set | 21.73 | 33.35 | 161.00 | 0.00 | 161.00 |
| Validation set | 24.20 | 33.88 | 161.00 | 0.00 | 161.00 |
| <i>Average SPT blow, N₂ (Corrected)</i> | | | | | |
| Training set | 18.60 | 22.32 | 161.00 | 0.00 | 161.00 |
| Testing set | 24.40 | 31.66 | 161.00 | 3.40 | 157.60 |
| Validation set | 25.62 | 32.10 | 161.00 | 0.00 | 161.00 |
| <i>Average SPT blow, N₃ (Corrected)</i> | | | | | |
| Training set | 26.83 | 26.17 | 161.00 | 0.00 | 161.00 |
| Testing set | 30.25 | 34.63 | 161.00 | 0.00 | 161.00 |
| Validation set | 31.87 | 34.97 | 161.00 | 0.00 | 161.00 |
| <i>Average SPT blow, N₄ (Corrected)</i> | | | | | |
| Training set | 31.71 | 27.56 | 195.00 | 2.69 | 192.31 |
| Testing set | 35.93 | 36.22 | 195.00 | 2.69 | 192.31 |
| Validation set | 37.06 | 37.18 | 195.00 | 2.69 | 192.31 |
| <i>Average SPT blow, N₅ (Corrected)</i> | | | | | |
| Training set | 39.17 | 34.43 | 250.00 | 4.13 | 245.87 |
| Testing set | 41.81 | 42.05 | 250.00 | 4.13 | 245.87 |
| Validation set | 43.63 | 43.71 | 250.00 | 4.13 | 245.87 |
| <i>Average SPT blow, N_{tip} (Corrected)</i> | | | | | |
| Training set | 47.87 | 53.33 | 300.00 | 0.00 | 300.00 |
| Testing set | 53.04 | 64.29 | 300.00 | 0.00 | 300.00 |
| Validation set | 55.81 | 66.59 | 300.00 | 0.00 | 300.00 |
| <i>Applied load, P (kN)</i> | | | | | |
| Training set | 6058.43 | 5804.45 | 40000.00 | 0.00 | 40000.00 |
| Testing set | 4094.59 | 4593.53 | 29400.00 | 0.00 | 29400.00 |
| Validation set | 4719.15 | 4480.86 | 25000.00 | 0.00 | 25000.00 |
| <i>Measured settlement, s_m (mm)</i> | | | | | |
| Training set | 12.36 | 17.89 | 185.00 | 0.00 | 185.00 |
| Testing set | 6.23 | 8.56 | 47.32 | 0.00 | 47.32 |
| Validation set | 10.36 | 17.96 | 137.50 | 0.00 | 137.50 |

^a Std. Dev. indicates standard deviation.

When a constant rate of penetration load test is performed, the measured pile settlement is an immediate settlement. However, in the case of a maintained load (ML) test, the measured settlement of the pile is a combination of immediate and consolidation settlement. In a typical ML test, the maximum time that the load is maintained is 72 h. However, the ML test data included in the database incorporates 140 (14%) measurements in clayey soil and 253 (25%) in sand, and only the clayey data are expected to include some proportion of consolidation settlement. Of the measured ML test settlement data in clayey soil, the database includes no measurements where the maximum time of load application was 72 h. In fact, the maximum load application time incorporated in the database is 20 h, and there are a total of 44 (4%) such data, and 45 (4%) where the load was maintained for less than one hour. Consequently, the amount of consolidation settlement included in the database is expected to be small and hence, the two pile load test types essentially measure immediate settlement.

To identify which of the input variables has the most significant impact on settlement predictions, a sensitivity analysis is carried out on the trained network. A simple and innovative technique proposed by Garson [14] is used to define the relative importance of the input variables by examining the connection weights of the trained network. Shahin et al. [37] illustrated the method for a neural network model with five inputs, two hidden layer nodes, and one output. In this paper, the method for the sensitivity analysis is carried out for a neural network model with 22 inputs (included the text variables), seven hidden layer nodes, and one output. The sensitivity analysis is repeated for networks trained with different initial random weights in order to test the robustness of the model in relation to its ability to provide information about the relative importance of the physical factors affecting pile settlement [37]. The results of the sensitivity analysis are discussed later.

4. Data division and pre-processing

It is common practice to divide the available data into two subsets; a training set, to construct the neural network model, and an independent validation set to estimate model performance in the deployed environment [42]. A modification of the above data division method is cross-validation [40] in which the data are divided into three sets; training, testing and validation. The training set is used to adjust the connection weights, whereas the testing set is used to check the performance of the model at various stages of training and to determine when to stop training to avoid over-fitting. The validation set is used to estimate the performance of the trained network in the deployed environment. Consequently, the database is divided into three sets; training, testing and validation. In total, 85.6% of the data (867 cases) are used for training and 14.4% (146 cases) are used for validation. The training data are further divided into 81% (701 cases) for the training set and 19% (166 cases) for the testing set.

Since it is essential that the data used for training, testing, and validation represent the same population [25], the statistical properties (e.g. mean, standard deviation and range) of the data subsets need to be similar [38]. In addition, it is generally accepted that ANNs perform best when they do not extrapolate beyond the range of their training data [12,41]. Consequently, in order to develop the best possible model, all patterns that are contained in the data need to be included in the training set. Similarly, since the test set is used to determine when to stop training, it needs to be representative of the training set and should therefore also contain all of the patterns that are present in the available data [37]. In this study in order to achieve this, several random combinations of the training, testing and validation sets are tried until three statis-

tically consistent data sets are obtained. The statistical parameters considered include the mean, standard deviation, minimum, maximum and range, as suggested by Shahin et al. [38]. Despite trying numerous random combinations of training, testing, and validation sets there are still some slight inconsistencies in the statistical parameters for each subset, as shown in Table 2. However, on the whole, the statistics are in good agreement and all three data sets may be considered to represent the same population.

After dividing the available data into their subsets, the variables are pre-processed by scaling them to a suitable form and to eliminate their dimension before they are applied to the ANN. The output variables need to be scaled to be commensurate with the limits of the transfer functions used in output layers [36]. Scaling the input variables is not necessary, so in this study the output variables are scaled between 0.0 and 1.0, as the sigmoid transfer function is used in the output layer.

5. Determination of model architecture

Determining the network architecture is one of the most important and difficult tasks in ANN model development [24]. It requires the selection of the optimum number of hidden layers and the number of nodes in each of these. There is no unified theory for determination of an optimal ANN architecture [36]. The number of nodes in the input and output layers are restricted by the number of model inputs and outputs. A total of 16 input variables are included in this study and, since the *NEUFRAME* software accepts text parameters, therefore instead of allocating a numeric value to these parameters, text parameters have been considered in the model development. It is noted that *NEUFRAME* allocates an input node for every one of the text parameters. For example, for the pile material, *NEUFRAME* allocates four nodes (one node each for Concrete, Steel, Composite, and Plastic). Therefore, the input layer of the ANN model developed using the *NEUFRAME* software contains 22 nodes, (two for the type of test [ML, CRP], four for pile material [Concrete, Steel, Composite, Plastic], two for method of installation [Replacement, Displacement], two for the pile tip [Closed, Open], and one for each of the input variables [EA , A_{tip} , O , L , L_{embed} , N_1 , N_2 , N_3 , N_4 , N_5 , N_{tip}]), and P . The output layer has a single node representing the measured value of settlement, s_m .

Although, it has been shown that a network with one hidden layer can approximate any continuous function [18], in this research a single and multiple hidden layers are used. In order to determine the optimum network geometry, first ANNs with a single hidden layer and 3, 4, 5, 6, 7, 8, 9, 10, 15, 20, 25, 30, 35, 40, 43, 44, and 45 nodes in the hidden layer are trained. It should be noted that 45 is the upper limit for the number of hidden layer nodes needed to map any continuous function for a network with 22 inputs, as discussed by Caudill [7]. Then ANNs with two, three and four hidden layers with different numbers of nodes in the hidden layers are trained.

Both models (single layer and multi-hidden layers) have been trained with a sigmoidal and a hyperbolic tangent (*tanh*) transfer function for the hidden layers. In the single hidden layer model, a sigmoidal transfer function is adopted for the hidden and output layers, and for the multi-hidden layers models, a *tanh* transfer function is used for the hidden layers and a sigmoidal transfer function is adopted for the output layer. These were combinations of transfer functions were found to yield the most accurate predictions of pile settlement when compared to the measured values.

6. Model optimization (training)

Training or learning is the process of optimizing the connection weights. The aim is to find a global solution to what is typically a

highly non-linear optimization problem [45]. The method most commonly used for establishing the optimum weight combination of feed-forward neural networks is the back-propagation algorithm [35], which is based on first-order gradient descent. Feed-forward networks trained with the back-propagation algorithm have already been applied successfully to many geotechnical engineering problems (e.g. [15,28]. Consequently, the back-propagation algorithm is used for optimizing the connection weights in this study. Details of the back-propagation algorithm can be found in many publications (e.g. [11]. In this work, the general strategy adopted for finding the optimal parameters that control the training process is as follows. A number of trials are carried out using the default parameters of the software used (i.e. the momentum term of 0.8 and a learning rate of 0.2). The network that performs best is then retrained with the different combinations of momentum terms and learning rates in an attempt to improve model performance. Since the back-propagation algorithm uses a first-order gradient descent technique to adjust the connection weights, it may get trapped in a local minimum if the initial starting point in the weight space is unfavourable [36]. Consequently, the model that has the optimum momentum term and learning rate is retrained a number of times with different initial weights until no further improvement occurs.

7. Stopping criteria

Stopping criteria are those used to decide when to stop the training process [37]. They determine whether the model has been optimally or sub-optimally trained [24]. Many approaches can be used to determine when to stop training, such as those described by [37]. As mentioned previously, the cross-validation technique [40] is used in this work as it is considered that sufficient data are available to create training, testing and validation sets and it is the most valuable tool to ensure over fitting does not occur [39]. The training set is used to adjust the connection weights, whereas the testing set measures the ability of the model to generalise and, using this set, the performance of the model is checked at many stages during the training process and training is stopped when the error of the testing set starts to increase [37].

8. Model validation

Once training of the model has been successfully accomplished, the performance of the trained model should be validated using data sets that have not been used as part of the learning process. This data set is known as the validation set. The purpose of the model validation phase is to ensure that the model has the ability to generalize within the limits set by the training data in a robust fashion, rather than simply having memorized the input-output relationships that are contained in the training data [37].

The coefficient of correlation, r , the root mean squared error, RMSE, and the mean absolute error, MAE, are the main criteria that are used to evaluate the prediction performance of ANN models. The coefficient of correlation is a measure that is used to determine the relative correlation between the predicted and measured data and can be calculated as follows:

$$r = \frac{C_{y_j d_j}}{\sigma_{y_j} \sigma_{d_j}}$$

$$C_{y_j d_j} = \frac{1}{n-1} \sum_{j=1}^n (y_j - \bar{y})(d_j - \bar{d})$$

$$= \frac{1}{n-1} \left(\sum_{j=1}^n y_j d_j - \frac{\sum_{j=1}^n y_j \sum_{j=1}^n d_j}{n} \right)$$

$$\sigma_{y_j} = \sqrt{\frac{\sum_{j=1}^n (y_j - \bar{y})^2}{n-1}}$$

$$\sigma_{d_j} = \sqrt{\frac{\sum_{j=1}^n (d_j - \bar{d})^2}{n-1}}$$

$$\bar{y} = \frac{\sum_{j=1}^n y_j}{n}$$

$$\bar{d} = \frac{\sum_{j=1}^n d_j}{n}$$

where y_j is the model (predicted) output; d_j is the desired (observed) output; $C_{y_j d_j}$ is the covariance between the model output (y_j) and the desired output (d_j); σ_{y_j} is the standard deviation of the model output y_j ; σ_{d_j} is the standard deviation of the desired output d_j ; \bar{y} is the mean of the model output y_j and \bar{d} is the mean of the desired output d_j ; and n is the number of data. Smith [39] suggested the following guide for values of $|r|$ between 0.0 and 1.0:

- $|r| \geq 0.8$ strong correlation exists between two sets of variables.
- $0.2 < |r| < 0.8$ correlation exists between the two sets of variables.
- $|r| \leq 0.2$ weak correlation exists between the two sets of variables.

The root mean square error, RMSE, is the most popular measure of error and it has the advantage that large errors receive much greater attention than small errors [16]. The root mean square error, RMSE, and mean absolute error, MAE, are desirable when the data evaluated are smooth or continuous [42].

9. Results

As mentioned previously, in this study two ANN models have been developed. The first model incorporates a single hidden layer and the second model utilizes multiple hidden layers. In order to determine the optimum network geometry, ANNs with a single hidden layer and 3, 4, 5, 6, 7, 8, 9, 10, 15, 20, 25, 30, 35, 40, 43, 44, and 45 nodes in the hidden layer are trained, then ANNs with two, three and four hidden layers with different numbers of nodes in the hidden layers are trained.

The results of the ANN with a single hidden layer and different numbers of nodes in the hidden layer are summarised in Table 3, assessed against the validation set. It can be seen that the network with seven hidden layer nodes has the lowest RMSE (12.42),

Table 3

Results for ANN model with a single hidden layer and different numbers of nodes for the validation set.

| Number of nodes in hidden layer | Correlation coefficient, r | RMSE (mm) |
|---------------------------------|------------------------------|-----------|
| 3 | 0.622 | 14.20 |
| 4 | 0.595 | 14.54 |
| 5 | 0.715 | 12.53 |
| 6 | 0.698 | 12.84 |
| 7 | 0.720 | 12.42 |
| 8 | 0.721 | 12.45 |
| 9 | 0.620 | 14.15 |
| 10 | 0.667 | 13.52 |
| 15 | 0.660 | 13.53 |
| 20 | 0.678 | 13.23 |
| 25 | 0.698 | 12.84 |
| 30 | 0.633 | 13.92 |
| 35 | 0.675 | 13.26 |
| 40 | 0.652 | 13.66 |
| 43 | 0.659 | 13.51 |
| 44 | 0.661 | 13.48 |
| 45 | 0.640 | 13.92 |

whereas the model with eight hidden layer nodes has the highest coefficient of correlation, r (0.721). The results of these two models for the three data sets are shown in Tables 4 and 5. The plots of the measured versus predicted settlement, for these two models, are shown in Figs. 1 and 2, respectively for the validation and testing sets. The results indicate that the ANN model with a single hidden layer performs unsatisfactorily, because it predicts negative settlements in the low settlement region. Furthermore, the single hidden layer model has low correlation coefficients and high root mean square errors for the validation set.

The results of a sensitivity analysis for the model with a single hidden layer and seven nodes are shown in Table 6. As one would expect, it can be seen that the applied load (P), embedded length of pile (L_{embed}), and the soil properties have the most significant effect on the predicted settlement when the network is trained with different initial weights.

Table 4
Results of ANN model with a single hidden layer with seven nodes.

| Data set | Correlation coefficient, r | RMSE (mm) |
|----------------|------------------------------|-----------|
| Training set | 0.922 | 6.95 |
| Testing set | 0.818 | 6.55 |
| Validation set | 0.720 | 12.42 |

Table 5
Results of ANN model with a single hidden layer with eight nodes.

| Data set | Correlation coefficient, r | RMSE (mm) |
|----------------|------------------------------|-----------|
| Training set | 0.920 | 7.00 |
| Testing set | 0.802 | 6.52 |
| Validation set | 0.721 | 12.45 |

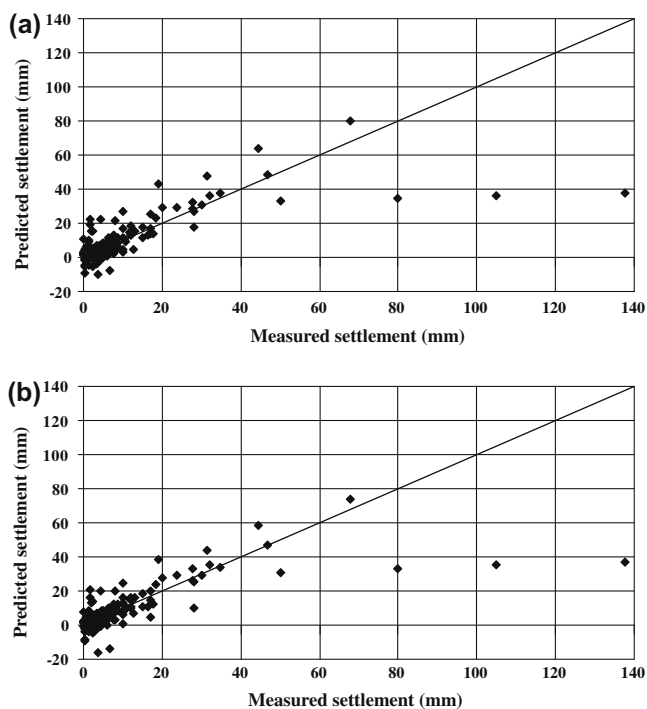


Fig. 1. Measured versus predicted settlements for the ANN models with a single hidden layer with respect to the validation set. Model with: (a) seven hidden layer nodes and (b) eight hidden layer nodes.

The results of the optimum networks for the multiple hidden layers are summarised in Table 7. It is observed that Model 14-6 is the optimum of the two hidden layer models, with 14 nodes in

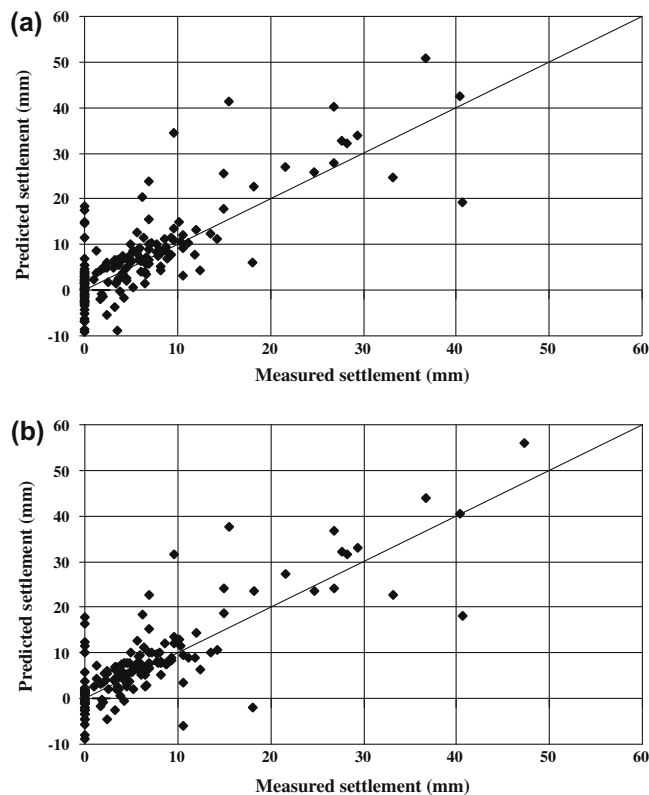


Fig. 2. Measured versus predicted settlements for the ANN models with a single hidden layer with respect to the testing set: (a) ANN model with seven hidden layer nodes and (b) ANN model with eight hidden layer nodes.

Table 6
Sensitivity analysis of the relative importance (%) of the ANN input variables.

| Input variables | Training no. | | | | Average |
|-----------------------------|--------------|-------|--------|-------|---------|
| | 1 | 2 | 3 | 4 | |
| <i>Type of test</i> | | | | | |
| ML | 3.47 | 5.19 | 4.42 | 4.15 | 4.59 |
| CRP | 3.28 | 2.96 | 3.9527 | 4.29 | 3.73 |
| <i>Type of pile</i> | | | | | |
| Concrete | 4.78 | 4.42 | 4.90 | 3.85 | 4.49 |
| Steel | 1.96 | 3.07 | 1.76 | 5.87 | 3.17 |
| Composite | 3.88 | 3.05 | 2.87 | 3.59 | 3.35 |
| Plastic | 2.93 | 2.57 | 3.35 | 1.88 | 2.68 |
| <i>Type of installation</i> | | | | | |
| Replacement | 4.70 | 2.15 | 2.98 | 4.62 | 3.61 |
| Displacement | 4.59 | 4.47 | 5.19 | 3.97 | 4.56 |
| <i>End of pile</i> | | | | | |
| Closed | 3.73 | 3.77 | 3.64 | 2.97 | 3.53 |
| Open | 3.30 | 3.41 | 4.19 | 3.20 | 3.53 |
| <i>Numerical variables</i> | | | | | |
| EA | 5.74 | 6.23 | 4.56 | 4.03 | 5.14 |
| A_{tip} | 4.19 | 3.70 | 3.41 | 2.92 | 3.56 |
| O | 4.07 | 4.80 | 3.27 | 4.89 | 4.26 |
| L | 6.55 | 3.52 | 6.33 | 5.53 | 5.48 |
| L_{embed} | 8.74 | 8.51 | 8.93 | 8.11 | 8.57 |
| N_1 | 6.31 | 7.56 | 6.22 | 5.72 | 6.45 |
| N_2 | 3.13 | 3.37 | 4.10 | 3.36 | 3.49 |
| N_3 | 3.84 | 6.26 | 2.56 | 3.50 | 4.04 |
| N_4 | 4.03 | 3.60 | 2.59 | 3.78 | 3.50 |
| N_5 | 3.86 | 2.34 | 4.21 | 4.01 | 3.61 |
| N_{tip} | 1.52 | 3.75 | 2.81 | 5.09 | 3.29 |
| P | 11.38 | 11.32 | 13.79 | 10.66 | 11.79 |

the first hidden layer and six nodes in the second, and Model 13-8-3 is the optimum of the three hidden layer models, with 13 nodes in the first, 8 in the second and 3 in the third hidden layer. It can be seen that the best result is obtained by the four hidden layer model with 15-13-5-2 nodes in the four hidden layers.

The effect of the internal parameters controlling the back-propagation algorithm (i.e. momentum term and learning rate) on model performance (model with 15-13-5-2 nodes in the four hidden layers) is shown in Table 8. It can be seen that the best prediction was obtained with a momentum value of 0.6 and the optimum learning was found to be 0.4.

The plots of the measured versus predicted settlement for the validation and testing sets are shown in Fig. 3. The results indicate that the model performs well, with an r of 0.972, and a RMSE of

Table 7
Results of optimum multiple hidden layer networks.

| Optimum multiple hidden layer models | Correlation coefficient, r | RMSE (mm) |
|--------------------------------------|------------------------------|-----------|
| 14-6 | | |
| Training | 0.993 | 2.12 |
| Testing | 0.937 | 3.02 |
| Validation | 0.950 | 10.34 |
| 13-8-3 | | |
| Training | 0.993 | 2.10 |
| Testing | 0.949 | 2.74 |
| Validation | 0.930 | 7.00 |
| 15-13-5-2 | | |
| Training | 0.991 | 2.42 |
| Testing | 0.930 | 3.20 |
| Validation | 0.961 | 5.12 |

Table 8
Effect of varying momentum and learning rate on the optimum four hidden layer model with 15-13-5-2 nodes in the hidden layers.

| Learning rate | Momentum term | Performance measures | | | | | |
|---------------|---------------|------------------------------|--------------|--------------|-------------|-------------|-------------|
| | | Correlation coefficient, r | | | RMSE (mm) | | |
| | | T | S | V | T | S | V |
| 0.2 | 0.05 | 0.987 | 0.932 | 0.902 | 2.86 | 3.10 | 17.40 |
| 0.2 | 0.1 | 0.990 | 0.959 | 0.921 | 2.65 | 2.47 | 14.27 |
| 0.2 | 0.2 | 0.991 | 0.956 | 0.917 | 2.46 | 2.54 | 13.53 |
| 0.2 | 0.4 | 0.985 | 0.947 | 0.898 | 3.37 | 2.88 | 12.67 |
| 0.2 | 0.5 | 0.992 | 0.963 | 0.930 | 2.24 | 2.43 | 7.87 |
| 0.2 | 0.6 | 0.991 | 0.947 | 0.966 | 2.49 | 2.81 | 4.91 |
| 0.2 | 0.7 | 0.989 | 0.961 | 0.942 | 2.93 | 2.59 | 6.39 |
| 0.2 | 0.8 | 0.991 | 0.930 | 0.961 | 2.42 | 3.20 | 5.12 |
| 0.2 | 0.9 | 0.989 | 0.938 | 0.955 | 2.63 | 2.97 | 5.31 |
| 0.2 | 0.95 | 0.992 | 0.952 | 0.596 | 2.42 | 2.83 | 14.45 |
| 0.05 | 0.6 | 0.992 | 0.959 | 0.955 | 2.40 | 2.44 | 7.30 |
| 0.1 | 0.6 | 0.992 | 0.963 | 0.917 | 2.20 | 2.33 | 11.83 |
| 0.3 | 0.6 | 0.987 | 0.966 | 0.930 | 2.94 | 2.28 | 6.78 |
| 0.4 | 0.6 | 0.993 | 0.958 | 0.972 | 2.17 | 2.47 | 4.49 |
| 0.5 | 0.6 | 0.990 | 0.962 | 0.968 | 2.63 | 2.44 | 5.63 |
| 0.6 | 0.6 | 0.990 | 0.922 | 0.943 | 2.59 | 3.42 | 6.34 |
| 0.8 | 0.6 | 0.984 | 0.870 | 0.887 | 3.58 | 4.77 | 8.42 |
| 0.9 | 0.6 | 0.991 | 0.927 | 0.903 | 2.71 | 3.67 | 7.97 |
| 0.95 | 0.6 | 0.990 | 0.925 | 0.934 | 2.61 | 3.45 | 6.56 |
| 0.99 | 0.6 | 0.980 | 0.872 | 0.848 | 4.69 | 5.88 | 9.79 |
| 0.05 | 0.8 | 0.992 | 0.960 | 0.915 | 2.30 | 2.42 | 12.12 |
| 0.1 | 0.8 | 0.992 | 0.940 | 0.953 | 2.46 | 3.13 | 5.49 |
| 0.3 | 0.8 | 0.988 | 0.930 | 0.945 | 2.98 | 3.31 | 6.15 |
| 0.4 | 0.8 | 0.989 | 0.931 | 0.951 | 2.77 | 3.18 | 5.59 |
| 0.5 | 0.8 | 0.981 | 0.896 | 0.880 | 4.04 | 4.89 | 8.98 |
| 0.6 | 0.8 | 0.980 | 0.889 | 0.907 | 3.92 | 4.94 | 7.59 |
| 0.8 | 0.8 | 0.992 | 0.941 | 0.881 | 2.23 | 3.01 | 8.81 |
| 0.9 | 0.8 | 0.991 | 0.914 | 0.948 | 2.53 | 3.49 | 5.93 |
| 0.95 | 0.8 | 0.990 | 0.924 | 0.962 | 2.53 | 3.28 | 4.87 |
| 0.99 | 0.8 | 0.972 | 0.812 | 0.889 | 7.52 | 8.52 | 9.24 |

T = training, S = testing, and V = validation.

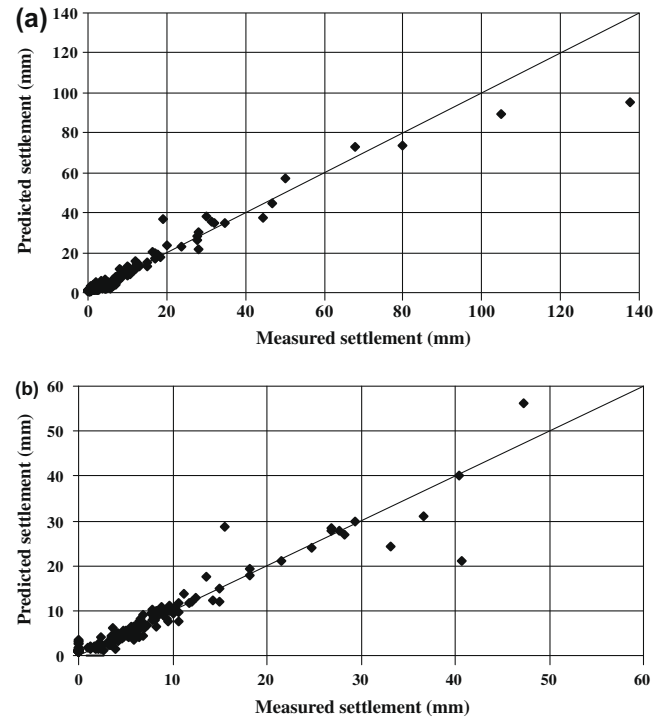


Fig. 3. Measured versus predicted settlements for ANN models with four hidden layers with 15-13-5-2 hidden layer nodes: (a) validation set and (b) testing set.

4.49 mm for the validation set, and 0.958 and 2.47 mm for the testing set. Whilst not particularly parsimonious, this is not the first time that an optimal ANN model has incorporated more than two hidden layers. For example, Karlik et al. [20] identified an optimal ANN model with 3 hidden layers for the vibration of a beam-mass system, which performed better than a single hidden layer model.

Comparisons between the results obtained from the optimal ANN model and four traditional methods commonly used to determine the settlement of piles are presented in the following section.

10. Numerical model

In this section an actual pile load test of a concrete pile is analyzed using the optimal ANN model (i.e. with 4 hidden layers and 15-13-5-2 nodes in the hidden layers), and the ANN predictions are compared with the measured settlement, as well as the results from four traditional methods: Poulos and Davis [33], Vesic [44], Das [8], and the non-linear t - z method proposed by Reese et al. [34]. The data for this pile were not included in the training set. The properties of the pile and soil are as follows: Type of test = maintained load (ML); type of soil = medium dense sand; type of pile = concrete; type of installation = bored; diameter of pile = 966 mm; length of pile = 11.4 m; embedded length of pile = 11.4 m; modulus of elasticity for pile = 31 GPa; the five corrected SPT N values along the embedded length of pile are: $N_1 = 32.82$, $N_2 = 18.95$, $N_3 = 18.88$, $N_4 = 16.24$, and $N_5 = 17.43$; and $N_{tip} = 17$.

11. Poulos and Davis [33] method

Poulos and Davis [33] suggested that the settlement of a pile, s , be determined using the following approach:

$$s = \frac{Pl}{E_s d}$$

where $I = I_0 R_K R_h R_v$ and is an influence factor for a rigid pile in a deep layer; I_0 is the settlement-influence factor for an incompressible pile in a semi-infinite mass, for $\nu = 0.5$; R_K is the correction factor for pile compressibility; R_h is the correction factor for finite depth, h , of layer on a rigid base and R_v is the correction factor for Poisson's ratio of the soil, ν . The parameters I_0 , R_K , R_h and R_v are obtained from a series of charts provided by Poulos and Davis [33].

12. Vesic [44] method

Vesic [44] suggested that the settlement of a pile, s , under a vertical working load, P_w , is the summation of three components s_1 , s_2 , and s_3 . Assuming the pile material to be elastic, the elastic compression of the pile itself, s_1 , is evaluated from:

$$s_1 = \frac{(P_{wp} + \zeta P_{ws})L}{A_{tip}E}$$

where P_{wp} is the load carried at the pile tip under working load conditions; P_{ws} is the load carried by skin resistance and ζ is a factor depending on the unit skin friction distribution. The settlement of a pile due to the load carried at the pile tip, s_2 , is expressed as:

$$s_2 = C_p \frac{P_{wp}}{dq_p}$$

where C_p is an empirical coefficient; and $q_p = 40 \frac{N_{tip}L}{d} \leq 400N_{tip}$ (kPa) [27].

And finally, the settlement of the pile caused by the load carried by the pile shaft, s_3 , is:

$$s_3 = C_s \frac{P_{ws}}{Lq_p}$$

where $C_s = (0.93 + 0.16\sqrt{\frac{L}{d}})C_p$.

The parameter ζ is assumed to equal 0.5 and the coefficient C_p is assumed to be equal to 0.09, as recommended for a sandy soil.

13. Das [8] method

The Das [8] method is the same as that proposed by Vesic [44], but with a slight difference to the evaluation of settlements s_2 and s_3 , as follows:

$$s_2 = \frac{P_{wp}d}{A_{tip}E_s}(1 - \nu^2)I_p$$

$$s_3 = \left(\frac{P_{ws}}{OL_{embed}}\right)\left(\frac{d}{E_s}\right)(1 - \nu^2)I_{ps}$$

where, $I_{ps} = 2 + 0.35\sqrt{\frac{L_{embed}}{d}}$.

The coefficient I_p is assumed to equal 0.88 for a pile of circular cross-section.

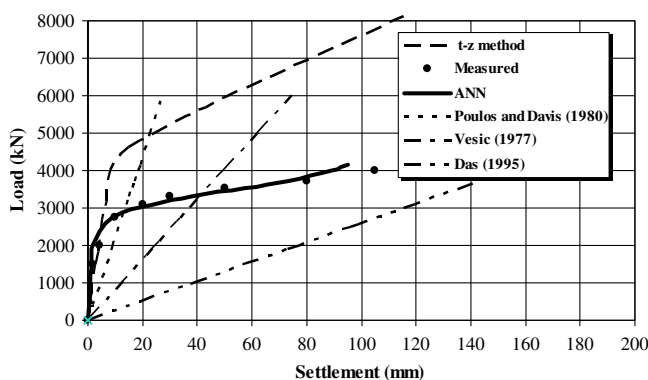


Fig. 4. Applied load versus measured and predicted settlements from the optimal ANN model, Poulos and Davis [33], Vesic [44], Das [8], and non-linear t - z methods.

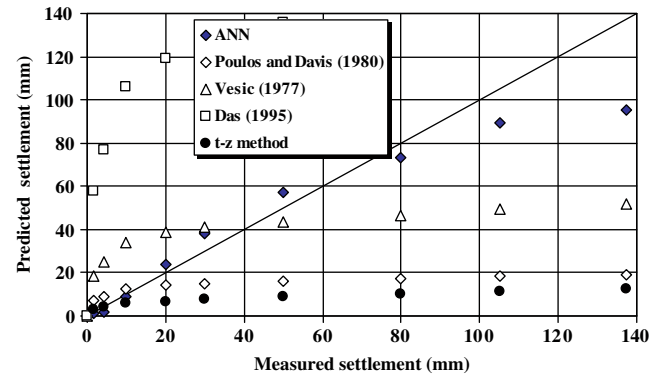


Fig. 5. Measured versus predicted settlements for the example pile for optimal ANN model; Poulos and Davis [33], Vesic [44], Das [8], and non-linear t - z methods.

Fig. 4 shows a plot of measured settlements [5] as a function of the applied load for the example pile, along with the settlements predicted by the optimal ANN model and the Poulos and Davis [33], Vesic [44] and Das [8] methods. In addition, in order to consider a non-linear load-settlement relationship (large displacement), the numerical example is also examined using of the t - z method of Reese et al. [34] by means of the *TZPILE* software, version 2.0. In addition, plots of measured versus predicted settlements for the example pile are shown in Fig. 5 for the optimal ANN model and the Poulos and Davis [33], Vesic [44], Das [8], and t - z methods. It can be seen that the ANN model satisfactorily predicts the measured data and significantly outperforms the traditional methods examined.

14. Conclusions

A back-propagation neural network was used to examine the feasibility of ANNs to predict the settlement of piles. A database containing 1013 case records of field measurements of pile settlements was used to develop and verify the model. The results indicate that back-propagation neural networks have the ability to predict the settlement of pile with an acceptable degree of accuracy ($r = 0.972$, $RMSE = 4.49$ mm) for settlements up to 185 mm. The ANN method has an additional advantage over conventional methods in that, once the model is trained, it can be used as an accurate and quick tool for estimating the settlement of piles.

Sensitivity analyses indicate that, as one would expect, the applied load (P), embedded length of pile (L_{embed}), and soil properties, in this case the SPT N value, have the most significant effect on the predicted settlement. The results of this study indicate that ANNs yield more accurate pile settlement predictions than those obtained from the traditional methods examined; namely those of Poulos and Davis [33], Vesic [44], Das [8], and the non-linear t - z method of Reese et al. [34]. The interested reader is encouraged to contact the first author for a copy of the optimal ANN model.

Acknowledgements

The authors would like to thank Richard Herraman and Peter Lai from the Departments of Transportation in Adelaide and Florida, respectively, and Keller Ground Engineering, UK for their assistance in providing access to some of their pile load test data.

References

- [1] Al-Homoud AS, Fouad T, Mokhtar A. Evaluating accuracy for two empirical methods in predicting settlement of drilled shafts. *Geotech Geol Eng* 2004;22:245–67.

- [2] Altaee A, Fellenius BH, Evgin E. Axial load transfer for piles in sand. I. Tests on an instrumented precast pile. *Can Geotech J* 1992;29:11–20.
- [3] Balakrishnan EG, Balasubramaniam AS, Phien-wej N. Load deformation analysis of bored piles in residual weathered formation. *J Geotech Geoenviron Eng ASCE* 1999;125(2):122–31.
- [4] Bowles JE. *Foundation analysis and design*. 5th ed. McGraw-Hill; 1996.
- [5] Briaud JL, Ballouz M, Nasr G. Static capacity prediction by dynamic methods for three bored piles. *J Geotech Geoenviron Eng ASCE* 2000;126(7):640–9.
- [6] Broms BB, Hellman L. End bearing and skin friction resistance of piles. *J Soil Mech Found Div, Proc ASCE* 1968;94(SM2):421–9.
- [7] Caudill M. *Neural networks primer, Part III*. *AI Expert* 1988;3(6):53–9.
- [8] Das BM. *Principles of foundation engineering*. 3rd ed. PWS Publ. Co.; 1995.
- [9] Fang HY. *Foundation engineering handbook*. New Delhi, India: CBS Publishers and Distributors; 2001.
- [10] Farquhar GB. Pile load tests at an Auckland industrial facility. In: *Proc of the 8th ANZ conference on geomechanics*, Hobart, 1; 1990. p. 383–7.
- [11] Fausett LV. *Fundamentals neural networks: architecture, algorithms, and applications*. Englewood Cliffs (NJ): Prentice-Hall; 1994.
- [12] Flood I, Kartam N. Neural networks in civil engineering I: principles and understanding. *J Comput Civ Eng* 1994;8(2):131–48.
- [13] Florida Department of Transportation (FDOT) (2003). Large diameter cylinder pile database. Research management center.
- [14] Garson GD. Interpreting neural-network connection weights. *AI Expert* 1991;6(7):47–51.
- [15] Goh ATC. Seismic liquefaction potential assessed by neural networks. *J Geotech Geoenviron Eng ASCE* 1994;120(9):1467–80.
- [16] Hecht-Nielsen R. *Neurocomputing*. Reading, Mass: Addison-Wesley; 1990.
- [17] Hirayama H. Load-settlement analysis for bored piles using hyperbolic transfer functions. *Soils Found* 1990;30(1):55–64.
- [18] Hornik K, Stinchcombe M, White H. Multilayer feed forward networks are universal approximators. *Neural Network* 1989;2:359–66.
- [19] Ismael NF. Analysis of load tests on piles driven through calcareous desert sands. *J Geotech Geoenviron Eng ASCE* 1999;125(10):905–8.
- [20] Karlik B, Ozkaya E, Aydin S, Pakdemirli M. Vibration of a beam-mass systems using artificial neural networks. *Comput Struct* 1998;69:339–47.
- [21] Liao SS, Whitman RV. Overburden correction factors for SPT in sand. *J Geotech Eng ASCE* 1986;112(3):373–7.
- [22] Lin SS, Hong JL, Lee WF, Chang YH. Capacity evaluation of static tested long piles. *Soil Dyn Earthquake Eng* 2004;24:829–93.
- [23] Lo SC, Li KS. Influence of a permanent liner on the skin friction of large-diameter bored piles in Hong Kong granitic saprolites. *Can Geotech J* 2003;40:793–805.
- [24] Maier HR, Dandy GC. Applications of artificial neural networks to forecasting of surface water quality variables: issues, applications and challenges. In: Govindaraju RS, Rao AR, editors. *Artificial neural networks in hydrology*. Dordrecht (The Netherlands): Kluwer; 2000. p. 287–309.
- [25] Masters T. *Practical neural network recipes in C++*. San Diego: Academic; 1993.
- [26] Meyerhof GG. Shallow foundations. *J Soil Mech Found Div Am Soc Civ Eng* 1965;91(SM2):21–31.
- [27] Meyerhof GG. Bearing capacity and settlement of pile foundation. *J Geotech Eng Div ASCE* 1976;102(GT3):197–228.
- [28] Najjar YM, Basheer IA. A neural network approach for site characterization and uncertainty prediction. *ASCE Geotech Spec Pub* 1996;58(1):134–48.
- [29] Ng CWW, Rigby DB, Ng SWL, Lei GH. Field studies of well-instrumented barrette in Hong Kong. *J Geotech Geoenviron Eng ASCE* 2000;126(1):60–73.
- [30] Omer JR, Robinson RB, Delpak R, Shih JKC. Large-scale pile tests in Mercia mudstone: data analysis and evaluation of current design methods. *Geotech Geol Eng* 2003;21:167–200.
- [31] Paik KH, Salgado R. Determination of bearing capacity of open-ended piles in sand. *J Geotech Geoenviron Eng ASCE* 2003;129(1):46–57.
- [32] Poulos HC. Common procedures for foundation settlement analysis—Are they adequate? In: *Proc 8th Australia New Zealand conf on geomechanics*, Hobart; 1999. p. 3–25.
- [33] Poulos HC, Davis EH. *Pile foundation analysis and design*. Wiley; 1980.
- [34] Reese LC, Isenhower WM, Wang ST. Analysis and design of shallow and deep foundations. John Wiley & Sons; 2006.
- [35] Rumelhart DE, Hinton GE, Williams RJ. Learning internal representation by error propagation. In: Rumelhart DE, McClelland JL, editors. *Parallel distributed processing, vol. 1*. Cambridge, Mass: MIT Press; 1986. Chapter 8.
- [36] Shahin MA. Use of artificial neural networks for predicting settlement of shallow foundations on cohesionless soil. PhD thesis, University of Adelaide; 2003.
- [37] Shahin MA, Maier HR, Jaksa MB. Predicting settlements of shallow foundations using artificial neural networks. *J Geotech Geoenviron Eng ASCE* 2002;128(9):785–93.
- [38] Shahin MA, Maier HR, Jaksa MB. Data division for developing neural networks applied to geotechnical engineering. *J Comput Civ Eng ASCE* 2004;18(2):105–14.
- [39] Smith M. *Neural networks for statistical modelling*. New York: Van Nostrand-Reinhold; 1993.
- [40] Stone M. Cross-validatory choice and assessment of statistical predictions. *J Roy Stat Soc B* 1974;36:111–47.
- [41] Tokar SA, Johnson PA. Rainfall-runoff modeling using artificial neural networks. *J Hydrol Eng* 1999;4(3):232–9.
- [42] Twomey JM, Smith AE. Validation and verification. In: Kartam N, Flood I, Garrett JH, editors. *Artificial neural networks for civil engineers: fundamentals and applications*. New York: ASCE; 1997. p. 44–64.
- [43] US Department of Transportation. A laboratory and field study of composite piles for bridge substructures. FHWA-HRT-04-043; 2006.
- [44] Vesic AS. Design of pile foundations. National cooperative highway research program, synthesis of practice No. 42. Washington, DC: Transportation Research Board; 1977.
- [45] White H. Learning in artificial neural networks: a statistical perspective. *Neural Comput* 1989;1:425–64.
- [46] Yang J, Tham LG, Lee PKK, Yu F. Observed performance of long steel H-piles jacked into sandy soils. *J Geotech Geoenviron Eng ASCE* 2006;132(1):24–35.
- [47] Zhang LM, Ng CWW, Chan F, Pang HW. Termination criteria for jacked pile construction and load transfer in weathered soils. *J Geotech Geoenviron Eng ASCE* 2006;132(7):819–29.